Channel estimation for a Mobile Terminal in a Multi-Standard Environment (LTE and DVB-H)

Foroughi, Farzad; Löfgren, Johan; Edfors, Ove

Published in:
3rd International Conference on Signal Processing and Communication Systems, 2009. ICSPCS 2009.

DOI:
10.1109/ICSPCS.2009.5306380

2009

Channel estimation for a Mobile Terminal in a Multi-Standard Environment (LTE and DVB-H)

Farzad Foroughi, Johan Lofgren, Ove Edfors
Dept. of Electrical and Information Technology, Box 118, Lund University, Sweden
Email: {Farzad.Foroughi, Johan.Lofgren, Ove.Edfors}@eit.lth.se

***Abstract*—In this paper, we present an analysis of different channel estimator structures that can be used and efficiently implemented with minor configuration changes of a common hardware for both LTE and DVB-H. Such common estimator structures for LTE and DVB-H allow algorithm and hardware reuse when both standards are implemented on the same platform. In this approach, a core estimator will be utilized to address parameter estimation for the two standards. The estimators exploit similarities in pilot patterns between LTE and DVB-H. The estimation techniques are discussed taking both algorithm and complexity issues into account.**

I. Introduction

Orthogonal Frequency Division Multiplexing (OFDM) is a special case of multi-carrier transmission and it can accomodate high data rate requirement of multimedia based wireless systems[1]. Due to its inherent structure, it is feasible to achieve a multiple-access format while benefiting from various coding and frequency hopping schemes. This will provide a high degree of diversity and inter-cellular interference suppression, etc. Another way of increasing the wireless system throughput is the employment of multiple antennas both on transmitter and receiver sides. Since parallel channels are established over the same time and frequency grid, high data rates without the need of extra bandwidth are achieved[1].This is known as Multiple Input Multiple Output (MIMO) in literature and has been the integral part of some recent state of the art wireless systems such as IEEE 802.11n and LTE.

In OFDM, the bandwidth is divided into a number of orthogonal narrow band subcarriers. The orthogonality of subcarriers is essential to OFDM which imposes some constraints on their spacing. The spacing should be smaller than the coherence bandwidth of the communications channel. An OFDM system is also prone to time variations of the channel. The system, however, is simple to implement and enjoys application of low complexity equalization techniques. Although equalization is rather simple especially when compared to non-OFDM communications systems, appropriate channel parameter estimation is still required to obtain the Channel State Information (CSI). Accurate CSI is crucial for resource allocation, adaptive modulation and coherent detection[2].

LTE is one of the evolved standards which promises a high consistent data rate over the wirless channels. It has already been adapted as the next generation standard for mobile communications. Similarly, DVB-H addresses the need for high multimedia data rates over the wireless communications channels. Operating in a multistandard enviroment mobile terminals are soon expected to be able to receive and decode data streams related to these two standards. Thus, it is desirable for them to accomodate the essential hardware/software to handle the requirements of the above mentioned standards. It is also envisaged that a typical terminal will have to decode and process multiple parallel streams corresponding to concurrent handling of LTE and DVB-H data at the same time. As a result, an increased amount of processing power needs to be provided while keeping the power efficiency as much as possible. Since the processing power cannot be surged indefinitely, novel low complexity algorithms need to be investigated in connection with the hardware desing. We have probed the channel estimation issues in the scope of this paper. More elaborately, new low complexity methods have been suggested which take both LTE and DVB-H standard requirements into consideration. Although the topic of channel estimation is both well-known and well-investigated to the communications community, the authors have not found many works which address designing flexible estimators that can be tailored to multistandard processing specifically to support coexisting of both LTE and DVB-H.

To assist channel estimation in DVB-H and LTE, scattered pilots have been allocated throughout the time-frequency grid as defined in the following sections. The pilot pattern is specific to each standard and largely depends on the typical environment the terminal experiences in parctice. Although there are differences in the way pilots are scattered for LTE or DVB-H, there are many similarities among them which can be exploited to develop a core estimator. Making good use of the similarities which arise from the inherent nature of the standards, common channel estimators can be developed. The proposed methods in this paper will rearrange the pilots in LTE and DVB-H in such a way they will look similar in structure. As a result, a number of flexible core estimators can be developed which can be equally applied to both standards with minor modifications in some parameters such as FFT size, number of pilots, etc.

II. Standards

The two different standards mentioned in the introduction have individually been designed based on the specific requirements of the environment they are to operate. Even though the standards are both based on OFDM, they embody major differences that need to be independently analyzed. In this section similarities and differences among the standards are highlighted from a channel estimation perspective. Important parameters of ineterest in this paper are the pilot patterns as well as resource allocations.

A. LTE (Long Term Evolution)

Mobile broadband encouraged the specification of LTE which became the basis for the next generation of UMTS Mobile standards[3]. The standard is intended for high data rates of at least 100Mbps in the downlink and 50Mbps in the uplink. It also constitutes flexible carrier bandwidth allocations from below 5MHz up to 20MHz[4] .

The entire downlink chain has been designed to decrease the receiver complexity. Several modes of operation have been designed to adapt to various channel enviromentes. The downlink chain in LTE has the following properties which are of considerable importance when it comes to channel estimation.

1) Downlink Frame Structure: A time-frequency representation of the available spectrum is called a resource grid[5], where the minimum unit is composed of one subcarrier in one symbol, named

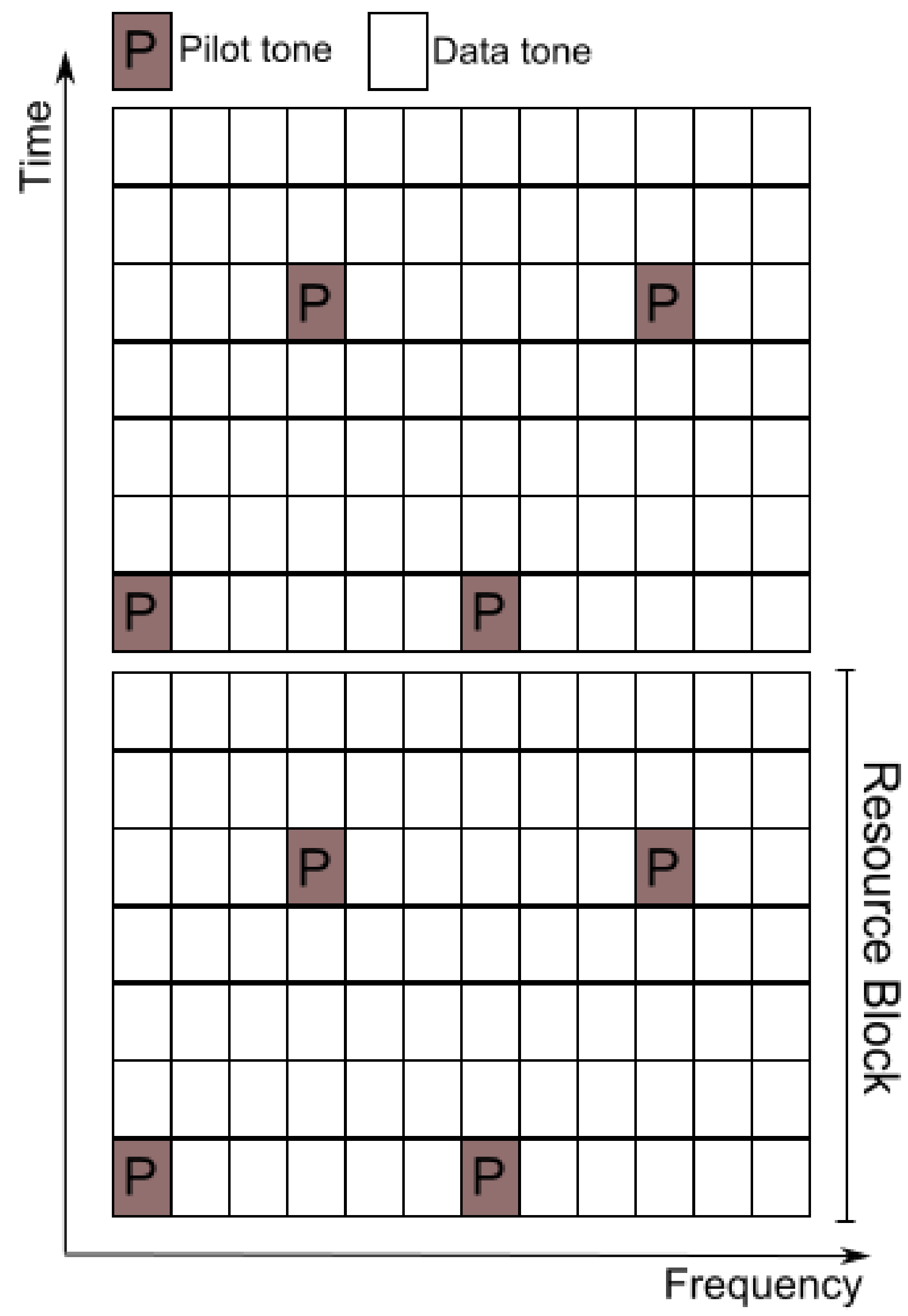

Fig. 1. LTE, time-frequency grid. Each box corresponds to one Resource Element(RE). A typical Resource Block is composed of 7 OFDM symbols in time and 12 subcarriers.

Resource Element (RE). Another important definition is physical Resource Block denoted as RB for simpilicity. An RB is a measurement in time and frequency corresponding to 6 or 7 OFDM symbols and 12 subcarriers, refer to Fig. 1.

2) Resource Allocations: LTE has a channel dependent scheduling[4]. This technique is specially tailored to the needs of low speed terminals. The specific resources are allocated to a terminal in relation to a channel condition measurement reported to the base station. There are three different formats for downlink scheduling assignments but only one of them supports frequency-contiguous allocation[4]. Generally, each terminal is guaranteed at least two consecutive RBs once the access to downlink data is granted. Fig. 1 shows the structure of two RBs and their relative location in the defined time frequency grid.

3) Pilot Pattern: LTE enjoys application of scattered pilots in the whole time-frequency grid. Being a MIMO system, LTE standardization has specified independent pilot patterns for each antenna port to facilitate parameter estimation. The LTE radio-access specifications refers to antenna ports rather than antennas to emphesize that what is refered to does not necessarily correspond to a single physical antenna[4]. Fig. 1 shows the pilot pattern for antenna port0[4]. Since scattered pilots do not cover the whole time-frequncy grid interpolation/extrapolation techniques should be practiced to derive a good channel estimate. The pilot patterns have been designed to address the need for a maximum attainable spectrum efficiency while satisfying the basic requirements for deriving a consistent channel estimate.

B. DVB-H (Digital Video Broadcasting-Handheld)

The Digital Video Broadcasting project (DVB) is an international industry-led consortium committed to the development of technical standards related to Multimedia broadcast. Being an evolution of DVB-T, DVB-H was specifically developed to address the needs of a low power mobile terminal. Some of the characteristics of DVB-H are as follows.

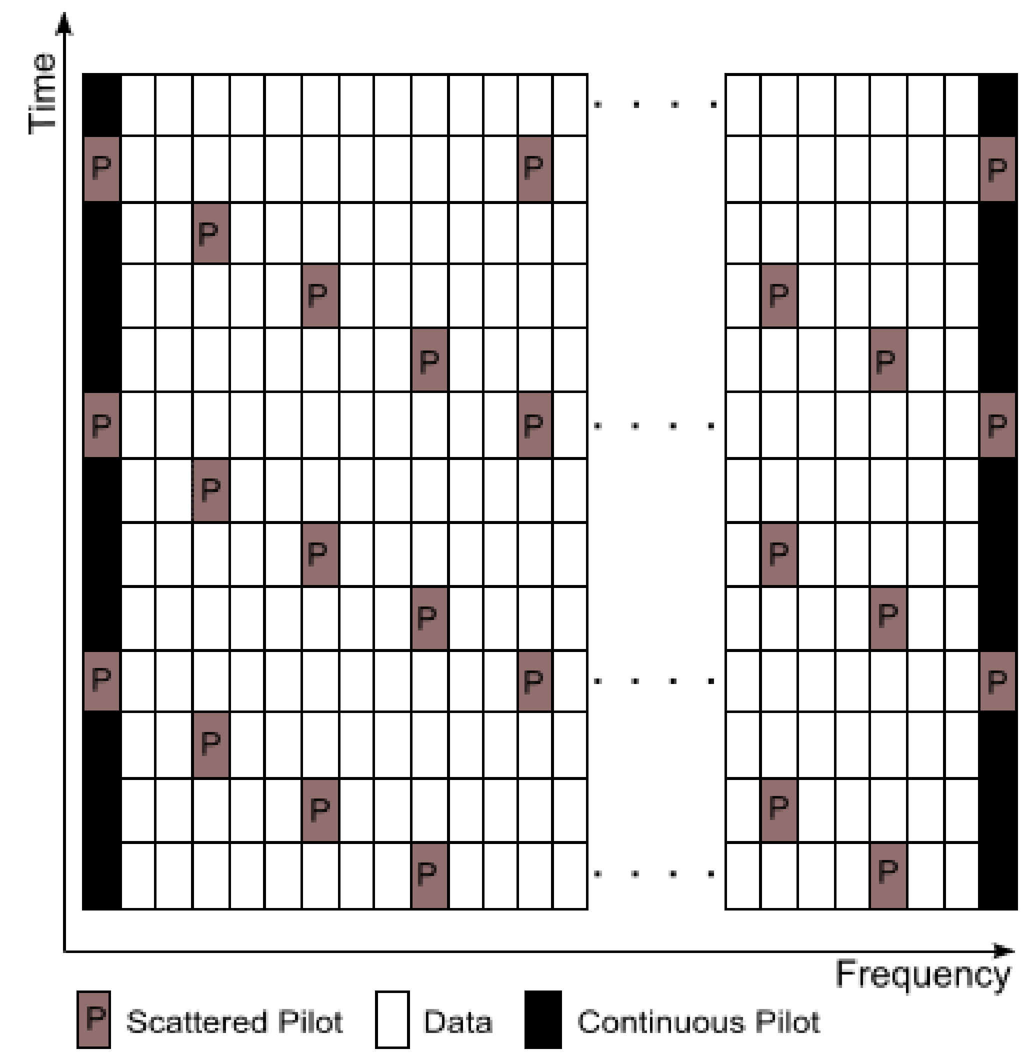

Fig. 2. DVB-H time-frequncy structure.

1) Frame Structure: DVB-H may operate in different modes, e.g. 2K, 4K, 8K. Irrespective of the mode of operation, one frame in DVB-H is defined to constitute 68 OFDM symbols[6]. DVB-H is in fact a broadcast standard and in contrast to LTE, all subcarriers in a symbol carry the information for all User Equipments (UEs). As stated earlier, in LTE data is individually allocated to UEs. Besides, each UE is guaranteed as few as 12 subcarriers in a given symbol.

2) Pilot Pattern: The pilots are intended to be used for time synchronization, frame synchronization, channel estimation, transmission mode identification and phase noise tracking. Both scattered as well as continuous pilots are transmitted in each symbol. While continuous pilots are primarily used for synchronization, scattered pilots are alloted for channel estimation purposes. Scattered and continual pilot structure are shown in Fig. 2

III. SYSTEM MODEL

Fig. 3 demonstrates a simple baseband OFDM system model. This general description of system fits any of the two standards being investigated in this paper without loss of generality. The uncoded data is modulated through one of the standardised modulation schemes (e.g. 4QAM) and placed on N_c parallel streams where N_c denotes the number of used subcarriers (excluding guard band). The combination of data and pilot subcarriers is fed into an IFFT block to finalise the OFDM modulation. The modulated data is passed through a fading channel with AWGN and OFDM demodulated through a FFT block at the other end. Demodulated data is further processed to decode the transmitted bit stream. To preserve the orthogonality of the subcarriers a Cyclic Prefix (not shown in this system model) with a length equal to the maximum expected delay spread is attached to the OFDM modulated data on the transmitter and discarded befor the demodulator on the receiver. We assume perfect synchronization at the receiving side. The data is fed to a channel estimator where data subcarriers indicated by white boxes in Fig. 1 and 2 need to be estimated using the available scattered pilots.

IV. CHANNEL ESTIMATION

Depending on the designated pilot pattern there are many approaches towards channel estimation for OFDM-based systems. Taking the fact that scattered pilots are standardised for the channel

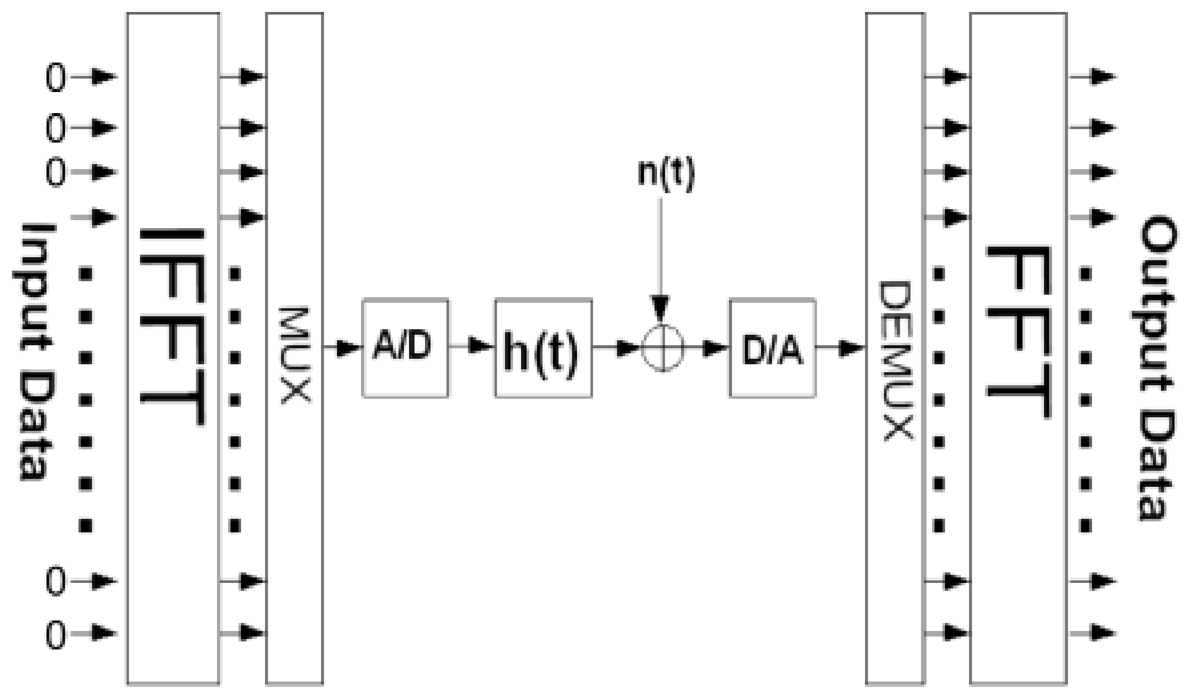

Fig. 3. The proposed system model. Zero padding is performed on both sides of input data vector on the subcarriers corresponding to the guard bands.

estimation in LTE as well as DVB-H into account, a number of estimation/interpolation techniques can be applied for channel estimation purposes in these systems. As already discussed in the previous section, Fig. 1 and 2 illustrate how the pilots are placed in the time-frequency grid for these two standards. Probably the best as well as the most complicated linear approach is the application of a 2-D Wiener filtering[7]. Yet, the mentioned estimator can be broken into two 1-D filters[7] to reduce the complexity. The 1-D filters correspond to seperate MMSE estimations one in time and the other in frequency directions. The estimation in time is a function of channel variations in time. The variantions of channel taps over time can be described by the Doppler spread, D_s. Meanwhile the Doppler spread shapes the spectrum[8] and affects the correlation properties of the channel taps over time. Thus, the coherence time (T_c) of a wireless channel can be defined as the interval over which the channel taps don't change significantly[9] given as,

$$T_c = \frac{1}{4D_s} \tag{1}$$

where D_s is the Doppler spread in the channel. This definition is a somewhat imprecise definition since the significant changes might belong to those taps which have lower energy[9] or vice versa. It is expected that the correlation between two realizations of a typical tap almost dissapears beyond the coherence time. Considering the restrictions wrapped around the coherence time, only the pilots in the vicinity of the estimated channel attenuations should be used. The time window in which the above mentioned method works shrinks as the Doppler spread increases. The Doppler spread can be described by the equivalent terminal speed relative to the transmitter (base-station). As the equivalent speed increases, the coherence time decreases which results in lower correlation among subsequent channel realizations. There are a number of proposed approaches to exploit the time correlation of various channel realizations. If the second-order channel statistics are known, MMSE methods can be used to estimate/interpolate the pilots in time. For instance, a robust MMSE estimator similar to the one applied for estimation in frequency (as described in the following sections) can be used in time as well.

In our proposed approach, however, we have resorted to a simple method which doesn't involve any estimations/interpolations in time. In fact, pilots from a number of neighboring symbols are collected and used to improve the channel estimation. This has been done presuming stationary channel enviroment and as a result works well in scenarios with low Doppler spreads. We have used the term mirrored pilots refering to the ones collected from the neighboring symbols and inserted to the pilot vectors used in the estimators. The mentioned pilot vectors as depicted in Fig. 4 and Fig. 5 also contain the existing pilots in each symbol.

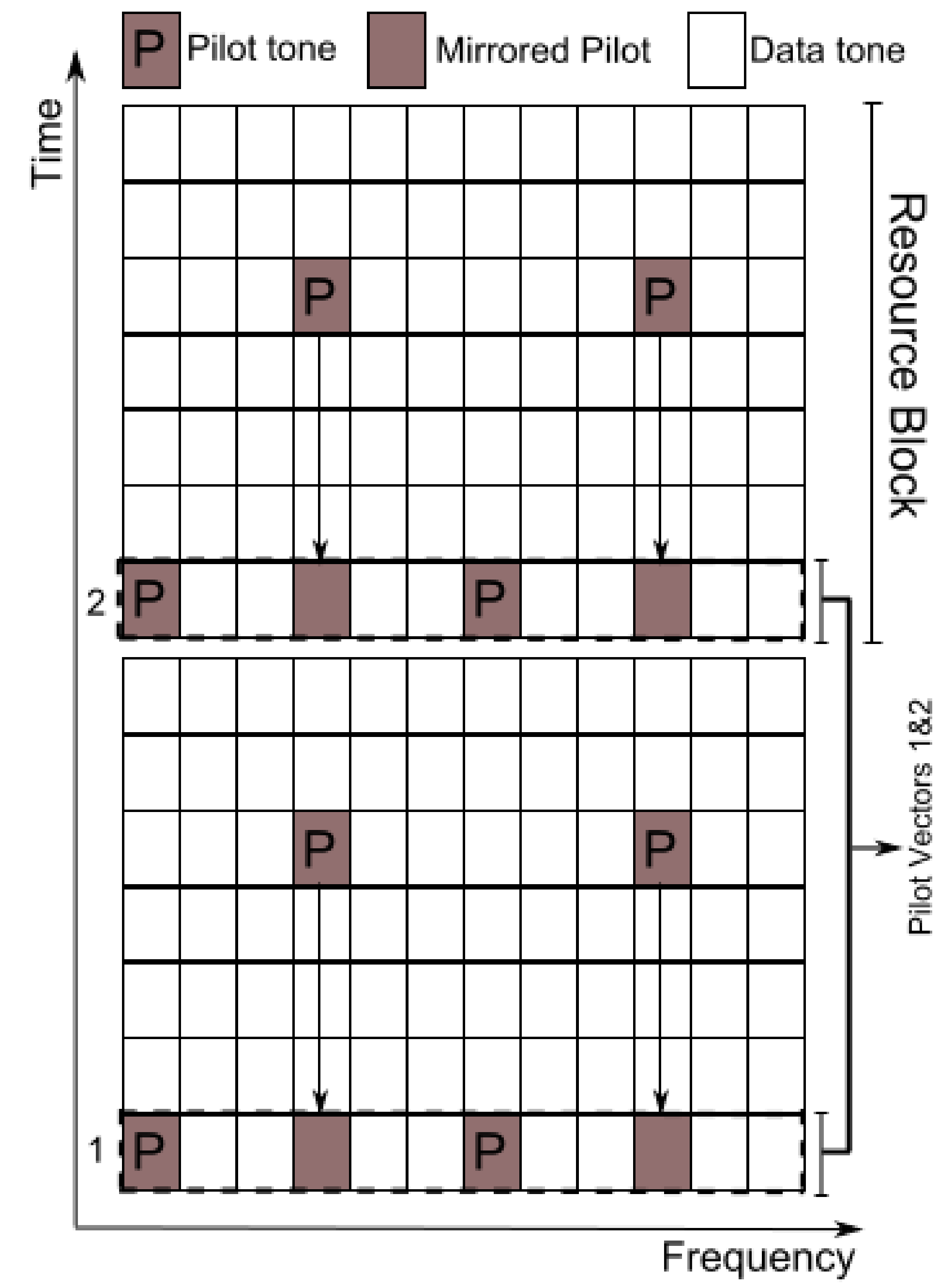

Fig. 4. LTE, time-frequnecy grid. Mirrored pilots are collected from other symbols to create the pilot vectors used in the estimators. Pilot vector 1 is used for estimation over all subcarriers in RB1 while pilot vector 2 is used for estimation over all subcarriers in RB2. The arrows indicate how the pilots from future symbols are reflected into the pilot vectors.

To carry out the estimation in LTE the pilots from symbols 1 and 5 in each RB are combined into a single pilot vector as depicted in Fig. 4. This pilot vector is subsequently fed into the proposed channel estimators. The derived estimation will be used for the whole OFDM symbols corresponding to that RB. Considering the definition of the coherence time as explained previously, it is expected that this method works for slow fading channels or in other words in channels characterised with low Doppler. Furthermore, the farther the pilots are located from a target symbol for estimation the lowest the cross-correlation they exhibit. As a result, the largest Mean Squared Error (MSE) is expected for OFDM symbol 7 in each RB, as it is furthest away from the pilots used in the estimation. Being the worst-case scenario, the derived Mean Squared Error as well as uncoded BER have been derived for symbol 7 as demonstrated in the simulations section.

The proposed approach is characterized with some drawbacks. For instance, data decoding for each symbol cannot initiate until the 5th symbol in each RB has been recieved and its pilots collected (mirrored). Thus, decoding has to be postponed until the pilot-assisted channel estimation is carried out using the pilots collected from symbols 1 and 5 in each RB. The associated memory overhead is expected to be acceptable specially for the noncontiguous resource allocation in LTE.

Similarly, to estimate a symbol in DVB-H, the pilots from other symbols are mirrored to fascilitate the channel estimation. In other words, the pilots from the past three OFDM symbols are saved in memory and consequently mirrored to the current symbol for the estimation purposes. Thus, the largest distance between the mirrord pilots and the current symbol is three OFDM symbols. Fig. 5 shows

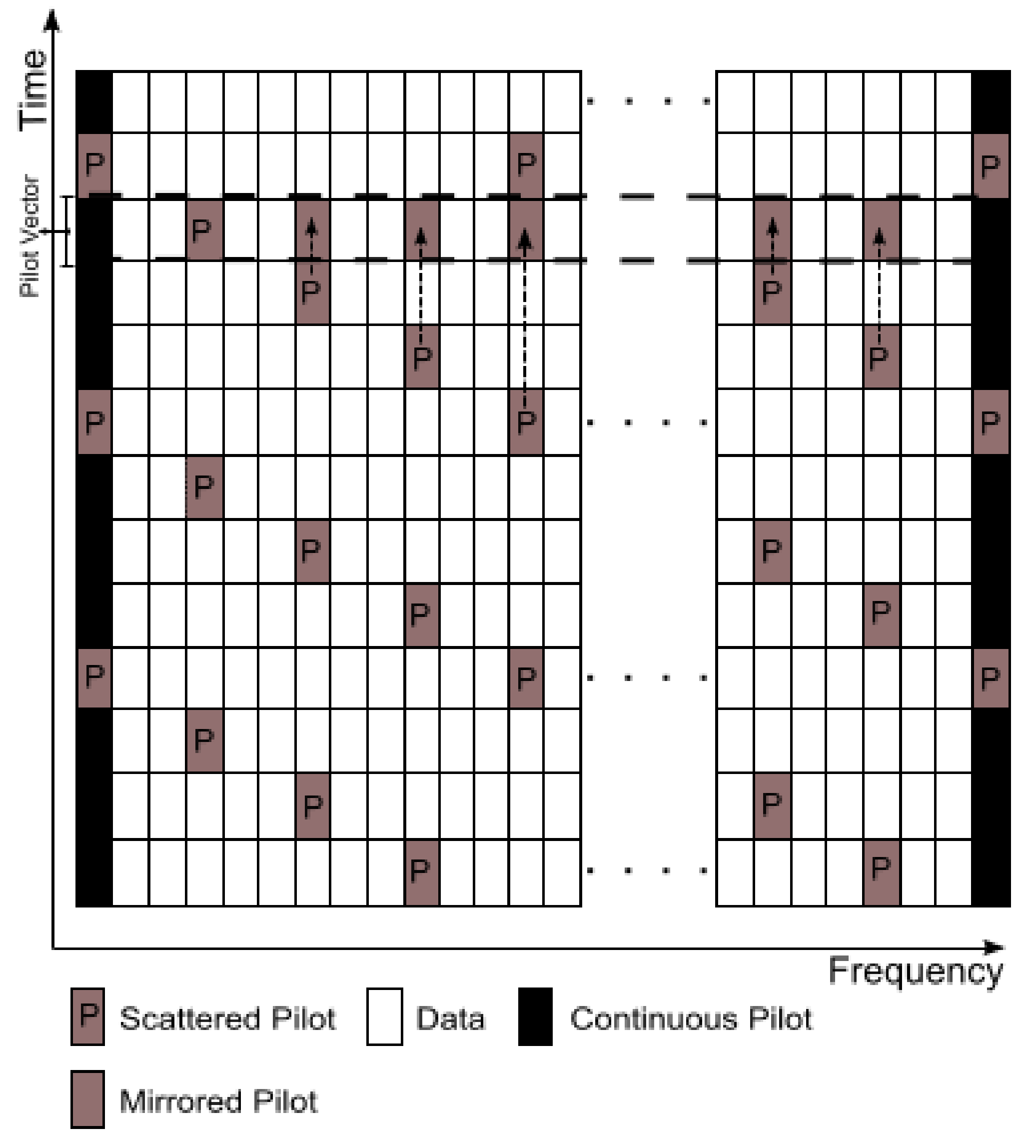

Fig. 5. DVB-H time-frequnecy structure. Mirrored pilots are collected from the past three symbols to create the pilot vectors used in the estimators. Contrary to LTE, each pilot vector in DVB-H is used to estimate only one OFDM symbol (the current symbol).

how the symbol identified by the dashed line is estimated through collection of pilots from the current as well as the past three symbols. It can be seen from the figure that the resulting pilot spacing in frequency will be three subcarriers after the appropriate pilots have been mirrored. This is quite similar to the witnessed pilot pattern in the attained pilot vector in LTE. Refer to Fig. 4 and Fig. 5 to see how the derived pilot vectors compare. In comparison to LTE, it is expected that application of this method to DVB-H doesn't affect the quality of the estimators as adversely in high Doppler scenarios. Besides, decoding of received symbols can immediately start (provided that the UE has already collected the pilots from the past three symbols) and the terminal doesn't need to wait for the additional pilots from the future symbols.

Having collected the desired pilots in time, data subcarriers need to be estimated in the frequency direction. Among the various investigated methods ML, MMSE[10] and DFT-based[11] estimators are examples of estimation algorithms. Our approach in this paper is the application of modified variants of MMSE and DFT-based estimators. There are benefits to simplified estimators for a low power mobile terminal due to the restricted amount of available processing power. If the estimators can benefit from the commonly available hardware on the platform, like FFT blokcs or baseband processors, allocation of extra resources dedicated to channel estimation becomes minimal.

A. MMSE estimator

The best linear estimator in terms of Mean Squared Error is the Linear Minimum Mean Squared Error Estimator (LMMSE)[7]. Given the transmitted symbols $\mathbf{X}$ and recieved symbols $\mathbf{Y}$, under certain conditions the simplified MMSE estimation of the channel $\mathbf{h}$ can be expressed as[12],

$$\hat{\mathbf{h}}_{mmse} = \mathbf{R}_{hh}(\mathbf{R}_{hh} + \frac{\beta}{SNR}\mathbf{I})^{-1}\hat{\mathbf{h}}_{ls} \tag{2}$$

where

$$\hat{\mathbf{h}}_{ls} = \mathbf{X}^{-1}\mathbf{Y} \tag{3}$$

is the Least Squares estimate of the channel attenuations $\mathbf{h}$, $\mathbf{R}_{hh}$ is the autocorrelation of the channel, $SNR = E|x_k|^2/\sigma^2$ is the signal-to-noise ratio and β is a constant which depends on the signal constellation of transmitted symbols, $\mathbf{X}$. For a 4QAM modulation scheme β equals 1.

In systems where scattered pilots are used to assist channel estimation the above equation may be rewritten as,

$$\hat{\mathbf{h}}_{mmse} = \mathbf{R}_{h_m h_p}(\mathbf{R}_{h_p h_p} + \frac{\beta}{SNR}\mathbf{I})^{-1}\hat{\mathbf{h}}_{p,ls} \tag{4}$$

where $\mathbf{X}_p$ and $\mathbf{Y}_p$ are the transmitted and received data sampled on the pilot positions and,

$$\hat{\mathbf{h}}_{pls} = \mathbf{X}_p^{-1}\mathbf{Y}_p \tag{5}$$

is the Least Squares estimate of the channel attenuations $\mathbf{h}_p$ on the pilot tones, $\mathbf{R}_{h_p h_p}$ is the autocorrelation of the sampled channel $\mathbf{h}_p$ on pilot positions and $\mathbf{R}_{h_m h_p}$ is the cross correlation matrix between the pilot tones and the data subcarriers.

The above equation system shows that for a channel containing N_p scattered pilots we need to have access to the second order channel statistics as well as the noise variance at any given time. Moreover, a matrix inversion of $N_p \times N_p$ should be carried out for any given SNR and a matrix calculation of $N_m \times N_p$ is required to the interpolation over N_m data subcarriers. Thus, this estimator exhibits considerable complexity[12].

B. Robust MMSE (R. MMSE) estimator

As its name implies, R. MMSE is designed to provide robustness of estimation for various channel realizations. It should provide an acceptable performance irrespective of the enviroment in which the UE is about to operate. For this purpose, the estimator could be designed for a worst-case scenario and its performance compared to the full MMSE. It can be shown[13] that this estimator peforms well under certain conditions. In this paper, we have chosen a uniform Power Delay Profile (PDP) where all the channel taps are equally strong. The length of the channel has been set to the length of the Cyclic Prefix. Consequently, the required correlation matrices , $\mathbf{R}_{h_m h_p}$ and $\mathbf{R}_{h_p h_p}$ can be precalculated. Meanwhile, it has been shown[12] that the performance loss is relatively acceptable for the lower SNRs if the estimator is designed for the maximum SNR the system is expected to experience in practice. Our simulation results also prove this point. Having fixed SNR in equation 4 the required matrices can be precalculated and stored in memory. Since large matrix inversions in 4 can be avoided the terminal can save a lot of processing as well as battery power. In fact, the R. MMSE estimator reduces the complexity to a mere matrix multiplication of size $N_m \times N_p$.

C. Modified Robust MMSE (M. R. MMSE) estimator

Channel estimation using a R. MMSE estimator makes use of all the pilot tones allocated to an OFDM symbol and is still a rather costly approach when it comes to hardware implementations. The implementation cost becomes even more crucial when the number of pilots grows like in 8K DVB-H mode of operation where each symbol constitutes at least 568 pilots. As a result, we have investigated alternative approaches to the R. MMSE estimator. To estimate each subcarrier only a few pilots in the vicinity of that subcarrier might be used. Fig. 6 illustrates how e.g. 8 pilots in the vicinity of two subcarriers k+10 and k+11 can be used and fed into the M. R. MMSE to carry out the channel estimation. In other words, exploiting the correlation for the full extent of the frequnecy axis might be of little use specially when the estimator is designed for a worst-case PDP.

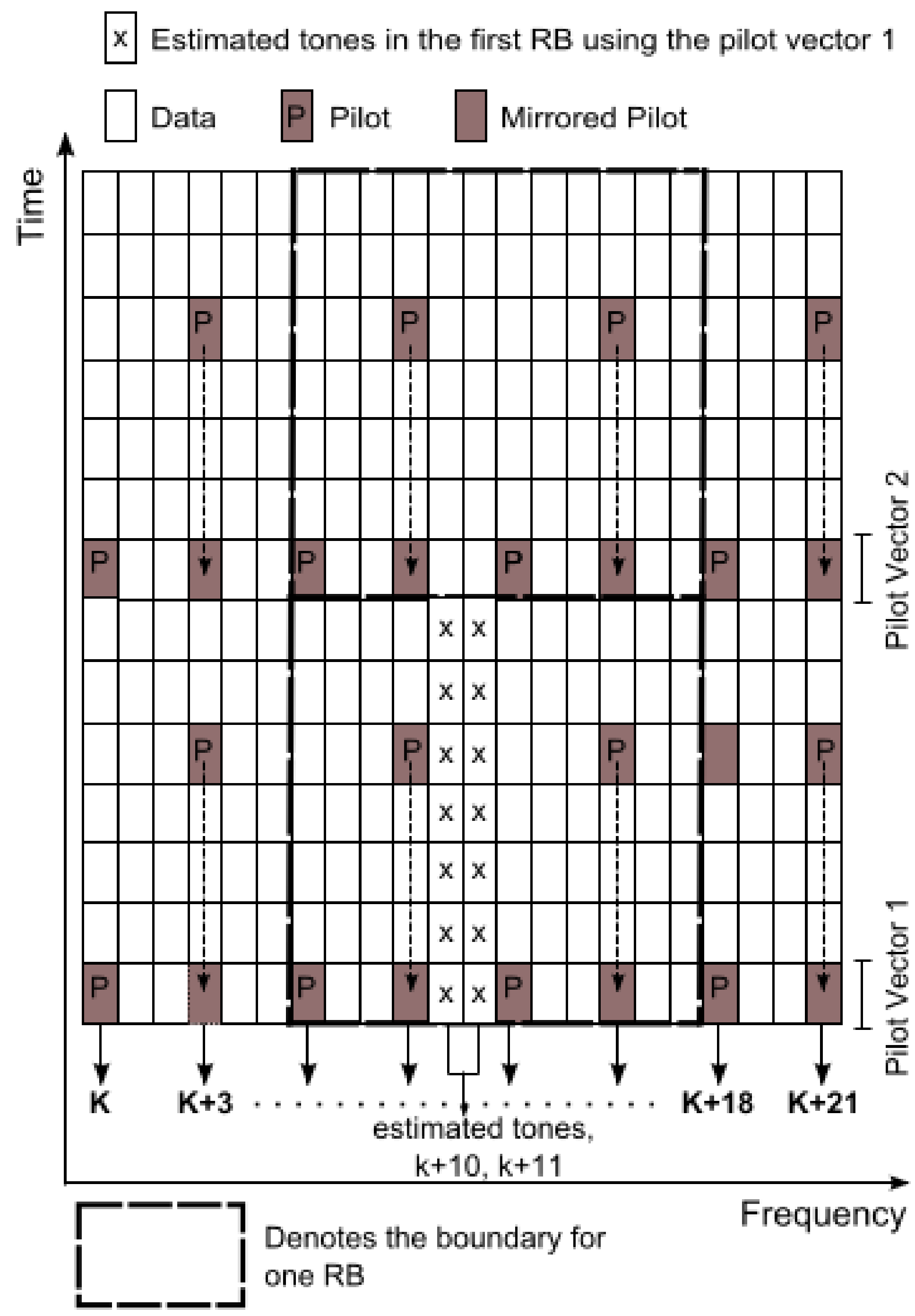

Fig. 6. Subcarrier estimation in LTE using only 8 pilots. Pilots from future symbols are mirrored to the current symbol to assist the channel estimation. The UE has access to all the pilots in each symbol irrespective of its allocated RBs. M. R. MMSE with 8 pilots can be used to carry out the estimation.

The autocorrelation of a system having a uniform PDP illustrates low correlation among subcarriers which are located far apart. We have exploited this feature to develop an estimator which uses only 16 neighboring pilots for estimation of each tone. As a result, in the proposed M. R. MMSE, $R_{h_p h_p}$ is a matrix of size 16×16. The pilots are preferebly selected symmetrical with respect to the estimated tone. As stated earlier, not only the pilots in the present symbol are used for estimation but also the pilots from other symbols as depicted in Fig. 4 and Fig. 5 are mirrored to improve the performance. This novel rearrangement of pilots proves to be performing well for low and medium terminal speeds. This has been proved through simulations as illustrated in the following sections.

D. DFT-based estimators

In OFDM systems where scattered pilots are used for channel estimation IDFT/DFT interpolation is one of the alternative approaches towards channel estimation. In these estimators the interpolation over all used subcarriers is obtained by[14],

$$\hat{\mathbf{h}}_{IDFT} = \frac{1}{N_p}\mathbf{F_L}\mathbf{F_P}^H\hat{\mathbf{h}}_{p,ls} \tag{6}$$

where N_p is the number of pilots $\mathbf{F}_L$ is a $N \times L$ matrix constructed by taking the first L columns of the full $N \times N$ fourier transform matrix and $\mathbf{F}_P$ is a subset of the fourier tarnsform matrix on the pilot positions where N is the FFT size of the system.Since the Least Squares approach is applied to obtain noisy estimations of the pilot subcarriers denoted as $\hat{\mathbf{h}}_{p,ls}$, the interpolation over all subcarriers will produce noisy estimates of the channel subbands. This will result in a relatively high noise floor which will end up in high Bit Error Rate after equalization. The associated error covarience matrix can be derived as[14],

$$\hat{\mathbf{C}}_{H_{IDFT}} \approx \frac{1}{N_p}{\sigma_{H_p}}^2\mathbf{F_L}\mathbf{F_L}^H \tag{7}$$

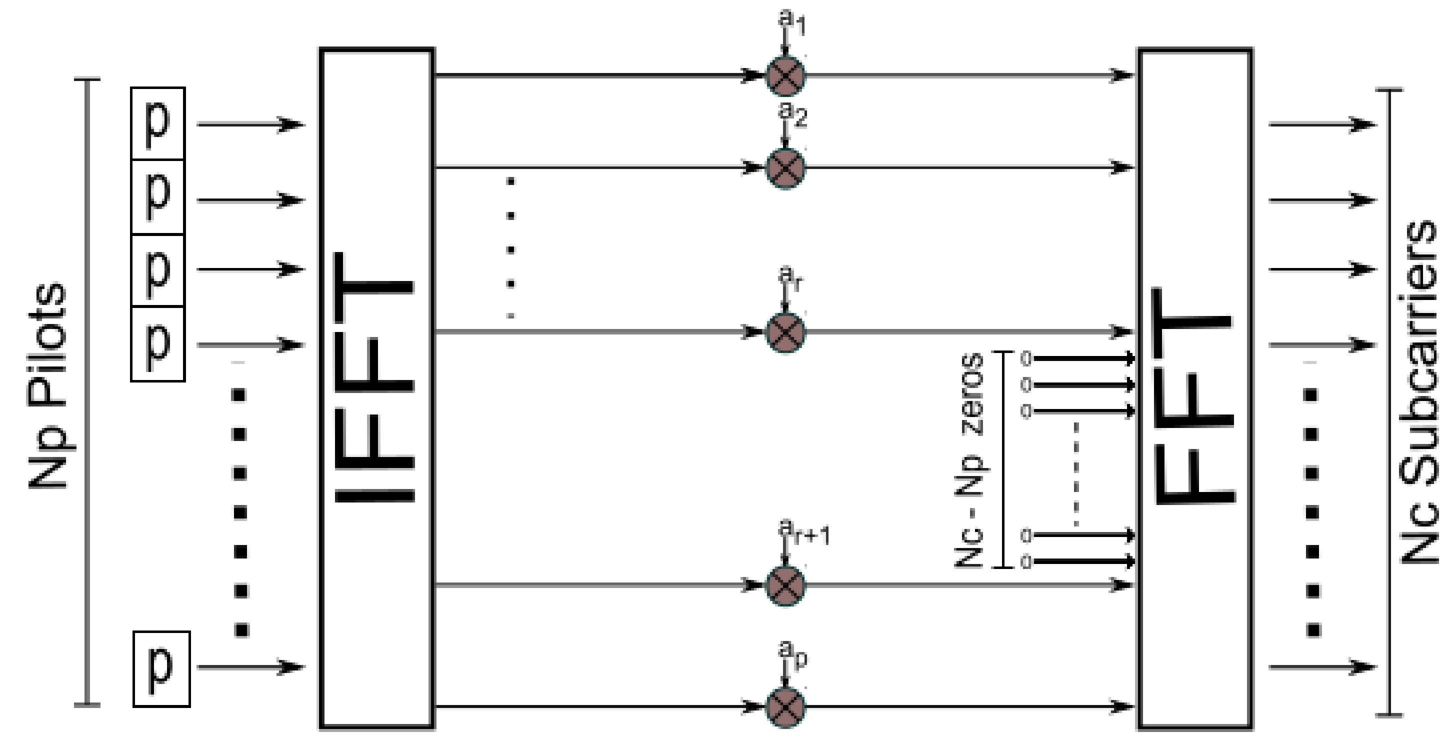

Fig. 7. The DFT-based estimator structure for the proposed estimators DFT-A, DFT-B, DFT-C. The elements in **a** will be all ones in case of DFT-A.

where ${\sigma_{H_p}}^2$ is the variance of the AWGN on the pilot subcarriers. The above equation indicates that the error covariance is a function of noise variance which will be reflected into the estimation results if no measures are taken to reduce its effect. Refered to as DFT-A estimator this method has been used in the context of channel estimation in this paper.

There are a handful of methods to remove the noise and decrease its variance in the system. One simple low complex way (we call that DFT-B estimator) is to capture the high energy taps of the channel after the IDFT and zero out the rest[11]. This is equivalent to a simple vector multiplication. The time-domain representation of noisy pilots fed into an IDFT of size N_p is,

$$\hat{\mathbf{g}}_{ls} = IDFT(\hat{\mathbf{h}}_{p,ls}) \tag{8}$$

Furthermore, the estimated channel can be described as,

$$\hat{\mathbf{h}}_{IDFT} = DFT(\hat{\mathbf{g}}_{ls} \times \mathbf{a}) \tag{9}$$

where vector $\mathbf{a} = [a_1 a_2 ... a_p]$ is a smoothing vector and the DFT size is equal to the number of used subbands, N_c as depicted in Fig. 7. Due to the nature of wireless channels the energy is usually concentrated in the first few taps. In case of sample-spaced channels the energy is perfectly confined in a limited area in the begining of the CIR. In case of the nonsample-spaced channels, part of this energy is leaked outside this area[11]. If the energy is confined to an area corresponding to the first r taps and the last q taps(which is due to cyclic nature of the DFT), the elements in vector $\mathbf{a}$ will be modified as follows,

$$\mathbf{a} = [a_1\ a_2 ... a_r\ 0\, 0 ... 0\ a_{p-q} ... a_p] \tag{10}$$

where all nonzero elements in the above vector will be equal to 1. Fig. 7 shows the general estimator structure we are using for our DFT-based estimators. The amount of time-domain processing after IDFT in DFT-B method is minor since it is limited to discarding the low energy channel taps and keeping the high energy ones[11].

Another low complexity DFT-based estimator (denoted as DFT-C estimator) is to weigth each channel tap by the following factor[11],

$$\frac{{\gamma_i}^2}{{\gamma_i}^2 + {\sigma_{H_p}}^2} \tag{11}$$

where ${\gamma_i}^2$ is the tap energy and ${\sigma_{H_p}}^2$ is the noise varaince. Thus, vector $\mathbf{a}$ will have N_p nonzero elements each corresponding to a weighting factor. This factor suppresses the noise energy on the channel taps and gives higher weight to useful signal energy. This estimator has a higher complexity compared to DFT-B which is propotional to the number of pilots. Weighting the taps in time-domain will introduce $3 \times N_P$ additional real multiplications compared to DFT-A and DFT-B. The performance/complexity trade-off, however, proves worthy specially when operating in lower SNR range as illustrated in the simulations section.

V. Hardware Implementation Issues

Due to the availability of FFT/IFFT blocks on an OFDM-based UE, it is beneficial to apply methods which might use the available hardware provided that it doesn't jeopardize its accessibility to more critical system components (e.g. OFDM demodulator, etc.). Since the focus of this paper is on algorithmic design, we will leave the detailed analysis of hardware implementation issues to future work. The nature of typical OFDM systems like LTE and DVB-H requires FFT transforms of sizes other than radix 2. Thus, the mixed-radix FFT blocks have to be used instead. A number of these FFT blocks have been proposed in litrature[15]. In this paper we have suggested application of a well-known mixed-radix Cooley-Tuckey algorithm which has the radices 2,3 and 5. This suffices the requirements of our proposed implementation for LTE and DVB-H. The block invloves the following computations for an FFT size of N[15],

$$N = 2^p \times 3^q \times 5^r \tag{12}$$

$$A(N) = 2N(\frac{3}{2}p + \frac{8}{3}q + 4r - 1) + 2 \tag{13}$$

$$M(N) = 2N(p + 2q + \frac{14}{5}r - 2) + 4 \tag{14}$$

$$A(N) + M(N) = 2N(\frac{5}{2}p + \frac{14}{3}q + \frac{34}{5}r - 1) + 2 \tag{15}$$

where $M(N)$ and $A(N)$ denote the number of real multiplications and additions. To measure the complexity of the proposed algorithms we have resorted to the corresponding number of required multiplications.

The above mentioned mixed-radix FFT suits the LTE DFT-based estimators without any further modifications. The number of pilots in different modes of LTE can be always broken into $N_p = 2^p \times 5^r$. Moreover, using the proposed pilot rearrangement in this paper the number of subcarriers will always be 3 times as many as the number of pilots which brings about the resulting number fed to the IFFT block being factorized into radices 2,3 and 5. Quite contrary to LTE, the standard number of pilots in DVB-H doesn't allow a mixed-radix FFT as mentioned above. For instance in 2K mode, the number of pilots in each symbol is 142 which after rearrangement (mirroring) the collected number of pilots in the pilot vector will be 568 that cannot be factorized into the desired radices (2,3 and 5). Thus, it is not possible to directly apply the desired FFT block in this paper for DFT-based channel estimation in DVB-H. To overcome this obstacle, we have extrapolated a minimum number of pilots outside the used band such that the resulting number of total pilots can be factorized into the desired radices. As a result, 8, 16 and 32 pilots (distributed symmetrically on each side of the used band) need to be extrapolated corresponding to 2K, 4K and 8K modes of operation in DVB-H. For the purposes of simulations in this paper we have resorted to the proposed MMSE channel estimation methods (M. R. MMSE) to extrapolate 8 pilots in the unused subband of DVB-H which makes the total number of pilots in the pilot vector be factorized as follows,

$$576 = 2^6 \times 3^2 \tag{16}$$

From a complexity overhead view point, the required additional processing for extrapolation is negligible compared to the whole. A comparison among the complexity requirements of the algorithms has been provided in the simulation section. We are, however, aware that to extrapolate the desired pilots, estimators with a better MSE performance exist compared to what we have applied here. These estimators can be precalculated and fetched from memory when needed. Yet, we have resorted to the estimators proposed in this paper since they provide acceptable performance as evidenced in the simulations section and eliminate the need for added complexity.

To address the computational needs of the MMSE-based algorithms, a pool of fast multipliers can be harnessed. In an efficient implementation each complex multiplication is carried out by 3 real multiplications. Similarly, a baseband processor can provide the necessary processing power. The mentioned resources are usually available as standard components on a typical OFDM-based UE and can be exploited for the purposes of channel estimation.

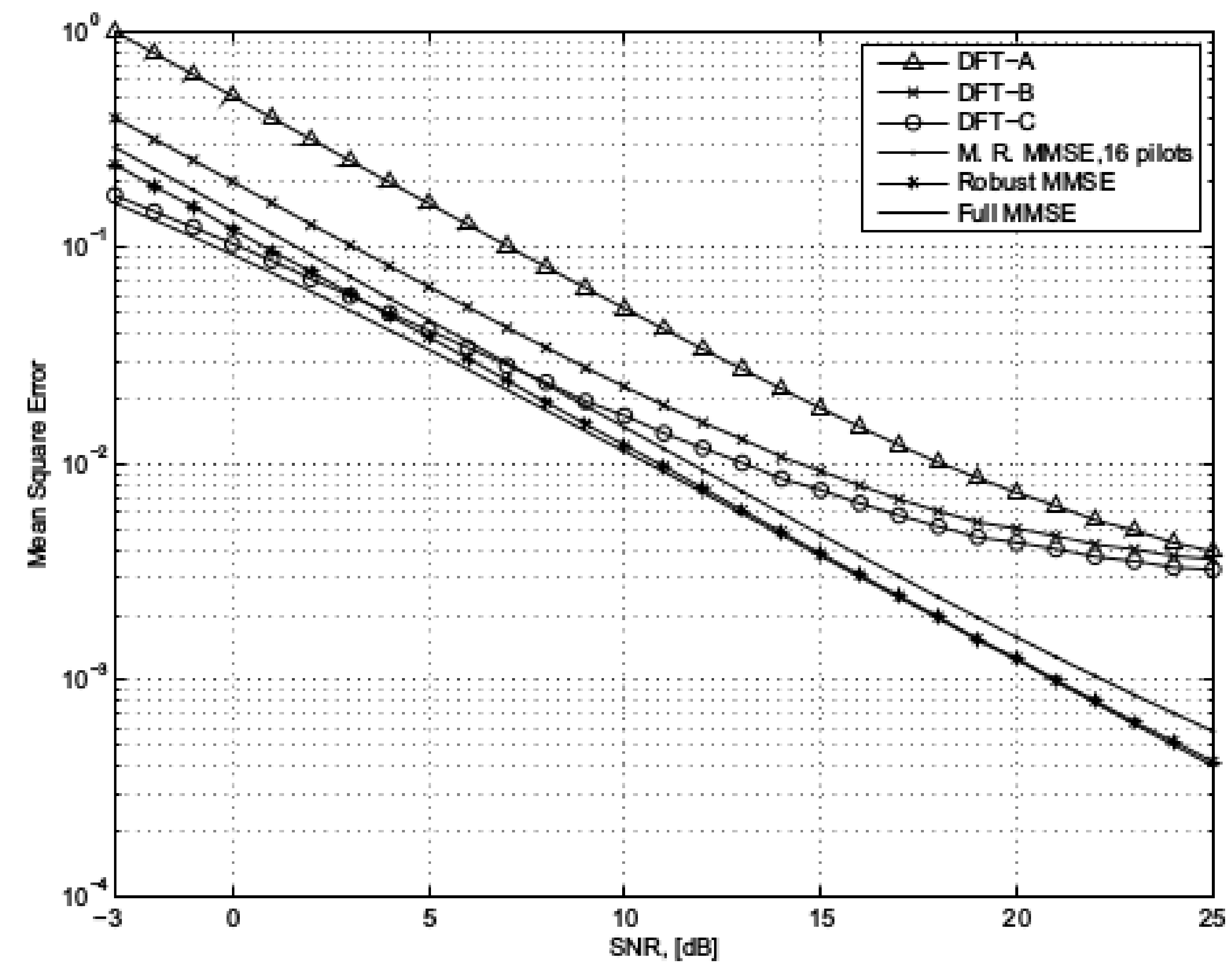

Fig. 8. LTE, MSE performance in a stationary environment.

VI. Simulation Results

A. LTE

The LTE simulation system parameters were chosen according to Table I.To illustrate the performance of the estimators, the widely

TABLE I
LTE,SIMULATED SYSTEM PARAMETERS

FFT size	512	$\delta f, [kHz]$	15
CP length,[n]	36	Used tones	300
Pilots/Symbol	50	PDP	$exp(-t/\tau_{rms})$
Carrier Freq.,[GHz]	2.6	Doppler Spec.	Two-dimensional, Jake's

used Mean Square Error as well as the Bit Error Rate measures have been used. Furthermore, no coding or interleaving schemes have been adopted. Thus, illustrated BERs correspond to uncoded data. Besides, the BER simulations have been carried out for a SISO system so that a fair comparison can be done among the performance of the estimators for both LTE and DVB-H. Fig. 8 shows how our estimators perform in a Mean Square Error sense for LTE.As mentioned earlier, full MMSE estimator is the best existing linear estimator. As a result, it has been selected as the reference against which other estimators are compared. As expected, DFT-A estimator has the worst performance amongst our proposed estimators due to its redundant noise varaince both in low and high SNRs. DFT-C performs best in low SNRs due to its capability to remove the additive noise and capture the useful energy of the channel taps. The R.

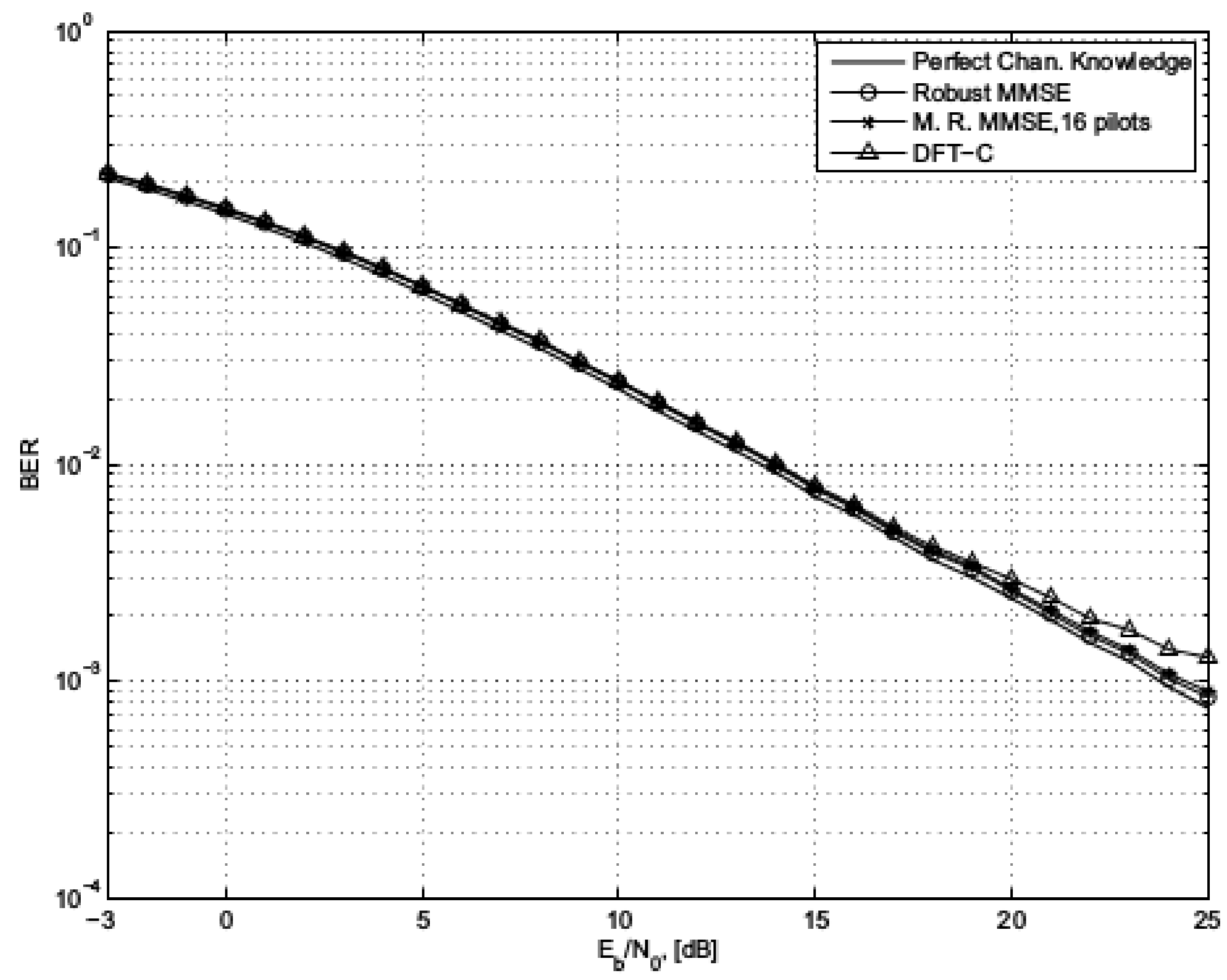

Fig. 9. LTE, uncoded BER performance for 4QAM in a stationary environment.

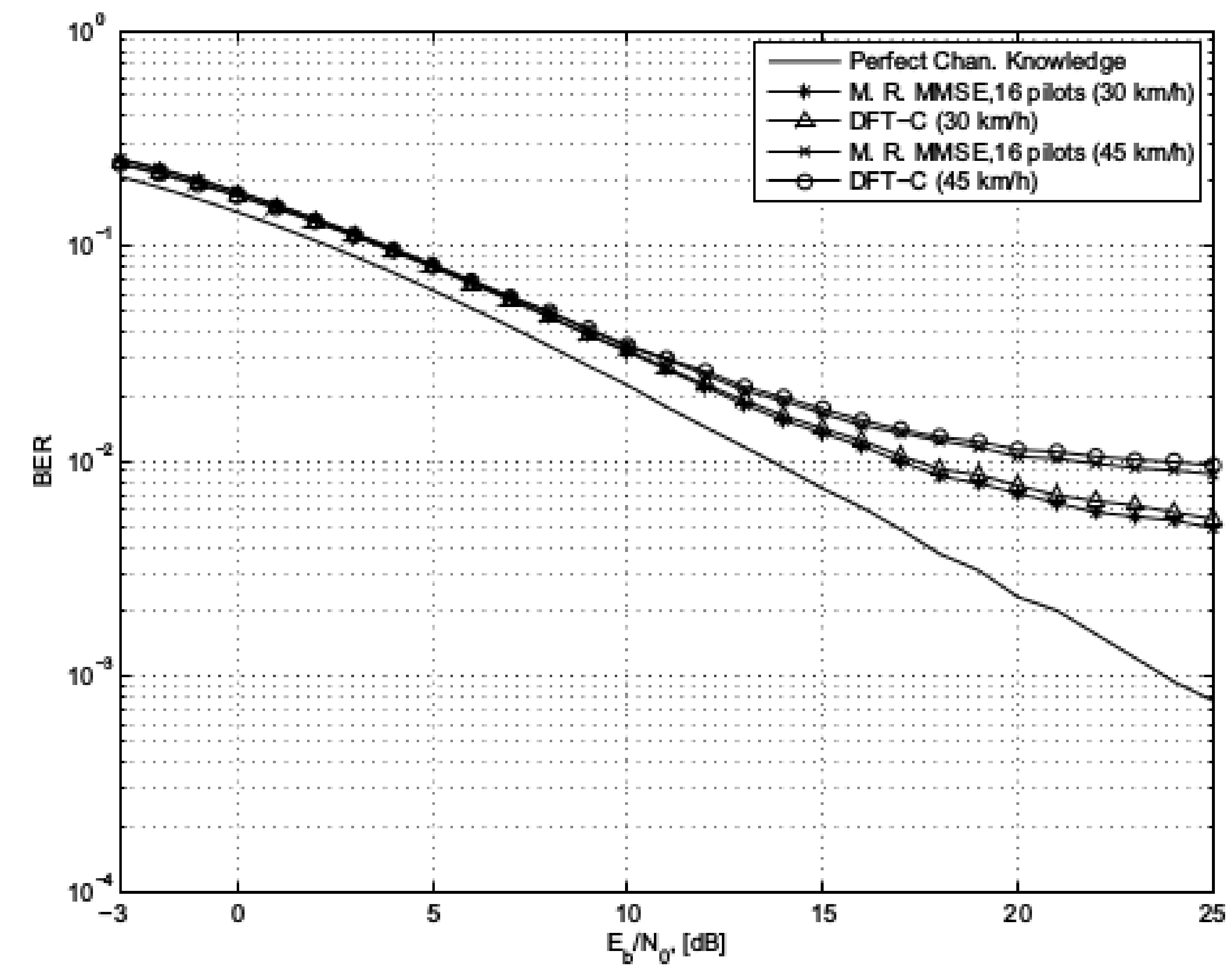

Fig. 10. LTE, uncoded BER performance for 4QAM corresponding to two different terminal speeds. Simulations have been done for OFDM symbol 7 in a typical RB which represents the worst-case scenario due to its low correlation with the constructed pilot vector.

MMSE as well as the M. R. MMSE estimators display an acceptable performance in the MSE sense over the whole SNR range.Having discarded DFT-A and DFT-B, Fig. 9 depicts the performance of DFT-C, R. MMSE and M. R. MMSE estimators from a BER view point. It can be seen that the vivid MSE differences occuring in the high SNR region shrink from a BER point of view when the simulations are done for 4QAM data modulation. The estimators have comparable performances for a stationary environment (no Doppler). Having a relativey equal performance, the R. MMSE can be also eliminated due to its complexity as elaborated in Table II. Figure 10 displays the BER performance of DFT-C and M. R. MMSE for two different enviroments. The enviroments have been simulated using the classical Jake's model[8][16] as a reference. The variations in this enviroment are simulated as an equivalent terminal speed. It can be seen that the decreased coherence in time can be partially compensated by increasing the Signal-to-Noise-Ratio. A quick look at Table III reveals the fact that it is not possible to maintain a target uncoded $BER = 10^{-2}$ when the terminal speed reaches a breaking threshold value.The result of our simulations suggest a terminal speed of around 50 km/h as the breaking value. Any attempts to sustain the uncoded BER above this speed fails even if the SNR is increased indefinitely. As discussed previously, the above mentioned effect is mainly the result of the correlation loss among realizations of channel taps due to the Doppler spread.

One should, however, consider the fact that the simulations have been done for the worst-case scenario (OFDM symbol 7) and it is expected that on average the breaking value for the terminal speed increases. For instance, our uncoded BER simulations for OFDM symbol 1 indicates a speed of 90km/h as the breaking threshold. We also know from experience that a mobile UE rarely operates in fast fading channels characterized by high terminal speeds and as a result a top speed of around 50 km/h satisfies the user needs in a majority of situations. It should also be pointed out that no coding/interleaving schemes have been used in the simulations and the system might perform better if the complete chain as standardised in LTE and DVB-H is implemented.

The complexity of DFT-based methods depend on the total number of available pilots corresponding to the LTE mode of operation. For the system simulated in this paper 100 scattered pilots have been used. Table II shows the required number of multiplications to estimate the

TABLE II
LTE, ESTIMATOR COMPLEXITY, NUMBER OF REAL MULTIPLICATIONS PER OFDM SYMBOL. N_{RB} REFERS TO THE NUMBER OF ALLOCATED RBS

Estimator	Total Complexity	Complexity Per RB
R. MMSE	75,000	3,000
M. R. MMSE	12,000	480
DFT-B	5,688	$\frac{5{,}688}{N_{RB}}$
DFT-C	5,988	$\frac{5{,}988}{N_{RB}}$

channel for the complete set of subcarriers corresponding to each OFDM symbol. The figures suggest that these estimators have a lower complexity compared to their MMSE counterparts. However, the overal cost of these estimators increases in the mean sense for LTE. The underlying reason can be described by the fact that the resource allocation in LTE is not always contiguous. As stated earler, as few as two consecutive Resource Blocks (RB) -one RB in each symbol- can be allocated to each terminal. That alone implies the redundancy of using the proposed DFT-based methods since they do the estimation over all subccariers in each symbol. On the other hand, M. R. MMSE estimator proves to provide a lower complexity in the mean sense since the complexity is a function of the number of estimated subcarriers (allocated RBs). The estimation complexity can be described and quantized on the basis of per Resource Block (RB). While the complexity of DFT-based estimator remains the same irrespective of the allocated number of subcarriers, the M. R. MMSE estimator's complexity can range from 480 to 12,000 multiplications per RB.

B. DVB-H

The DVB-H simulation system parameters were according to Table IV.

The simulation enviroment has been modeled similar to LTE except for the parameters which are specific to DVB-H like PDP length, etc. Furthermore, MSE as well as BER have been used as measures of estimator performance. Fig. 11 shows the MSE performance while

TABLE III
LTE, REQUIRED SNR TO MAINTAIN A CONSTANT UNCODED $BER = 10^{-2}$ FOR A NUMBER OF TERMINAL SPEEDS. SIMULATIONS ARE ASSOCIATED WITH OFDM SYMBOL 7 IN A TYPICAL RB. THE FIGURES HAVE BEEN DERIVED FROM M. R. MMSE SIMULATION RESULTS.

Speed, [km/h]	Doppler spread, [Hz]	SNR, [dB]
10	48	14.8
20	96	15
30	144	17
40	192	20
45	217	21
48	231	30
50	241	N.A.

TABLE IV
DVB-H, SIMULATED SYSTEM PARAMETERS

FFT size	2048	δf, $[kHz]$	4.464
CP length,[n]	63	Used tones	1704
Pilots/Symbol	142	PDP	$exp(-t/\tau_{rms})$
Carrier Freq.,[MHz]	500	Doppler Spec.	Jake's Spectrum

Fig. 12 displays the BER results for the proposed estimators in a stationary enviroment. Similarly, we can witness the quality of these estimators under varying channel conditions as depicted in Fig. 13. Analogous to LTE, we have investigated the BER breaking terminal speed for the proposed algorithms.The results in Table V expose us to the fact that these algorithms perform well for a larger range of terminal speeds when applied to DVB-H. This can be partly described by the lower carrier frequency in DVB-H as well as the used pilot structure. Contrary to LTE, DFT-based estimators provide lower complexity when compared to M. R. MMSE for DVB-H systems. This is largely due to the fact that DVB-H is a broadcast scheme in which each terminal needs to decode the entire subcarriers in each OFDM at a time. Thus, the terminal needs to estimate all the data subccariers to decode the recieved data. Table VI reveals the required complexity for each estimator. Hence, the DFT estimators provide a lower complexity in contrast with M. R. MMSE.

TABLE V
DVB-H, REQUIRED SNR TO MAINTAIN A CONSTANT UNCODED $BER = 10^{-2}$ FOR A NUMBER OF TERMINAL SPEEDS. THE FIGURES HAVE BEEN DERIVED FROM M. R. MMSE SIMULATION RESULTS.

Speed, [km/h]	Doppler spread, [Hz]	SNR, [dB]
10	9	14
50	46	14.8
100	92	15.4
150	139	17
190	176	22
200	185	24
210	194	N.A.

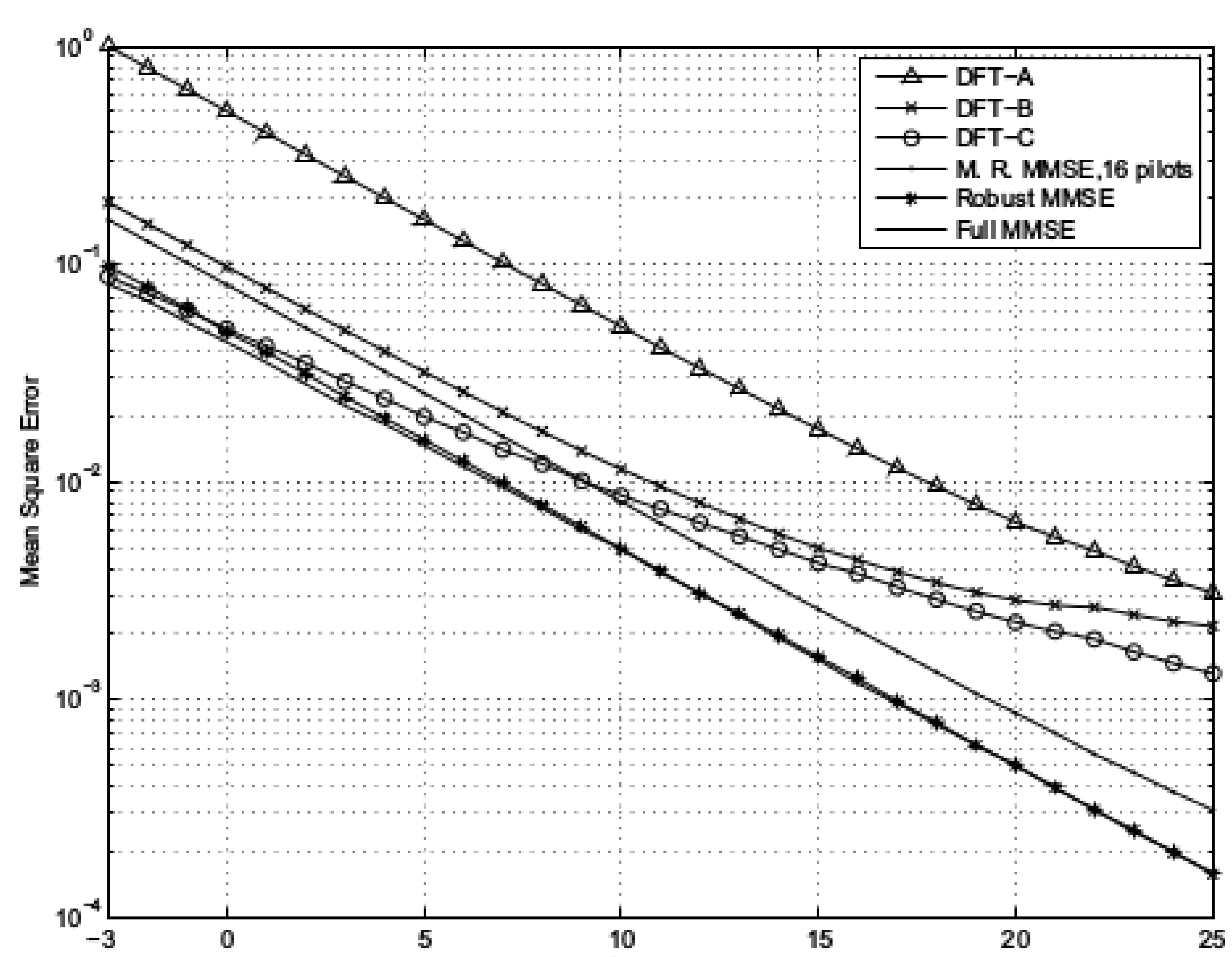

Fig. 11. DVB-H, MSE performance in a stationary environment.

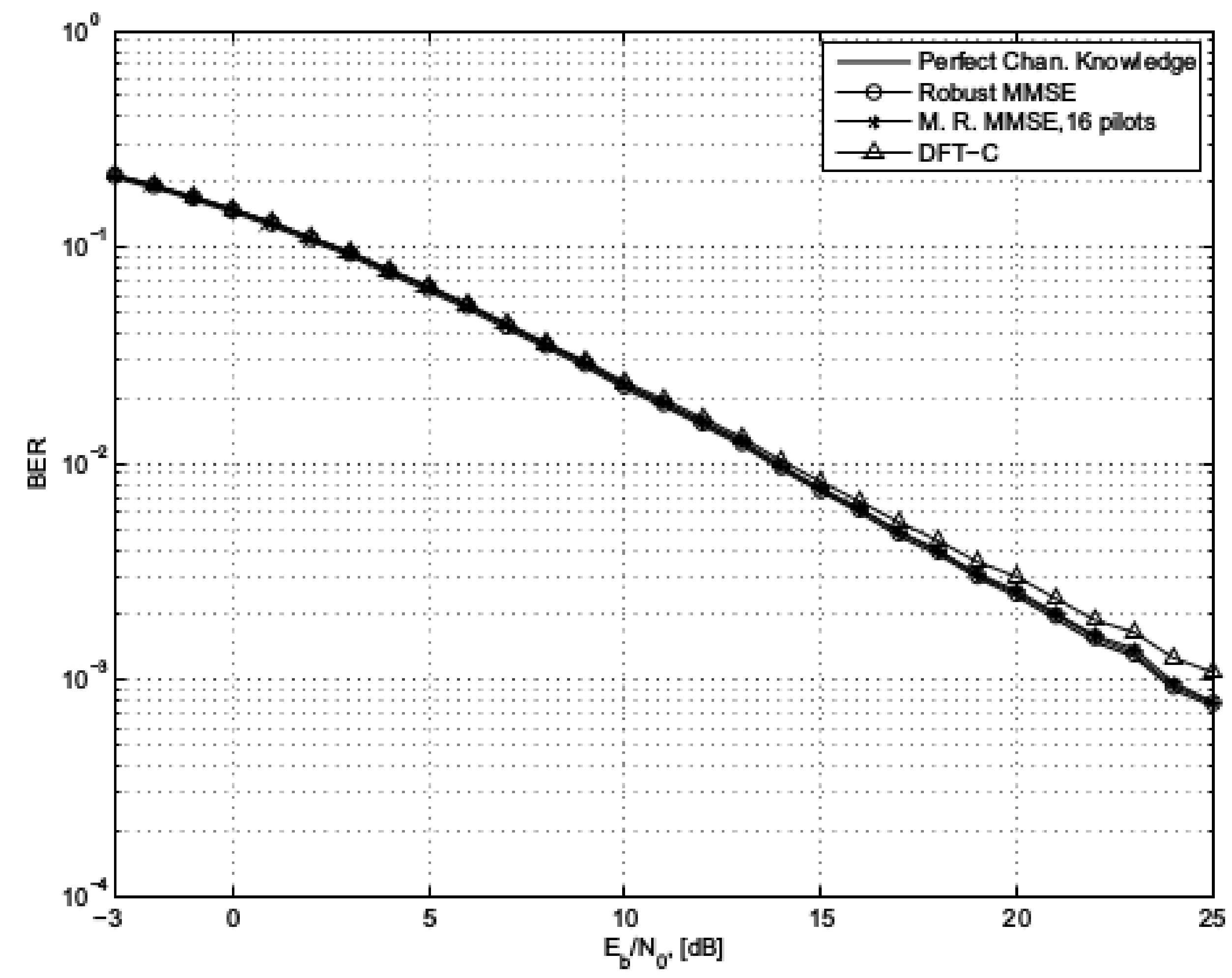

Fig. 12. DVB-H, uncoded BER performance for 4QAM in a stationary environment.

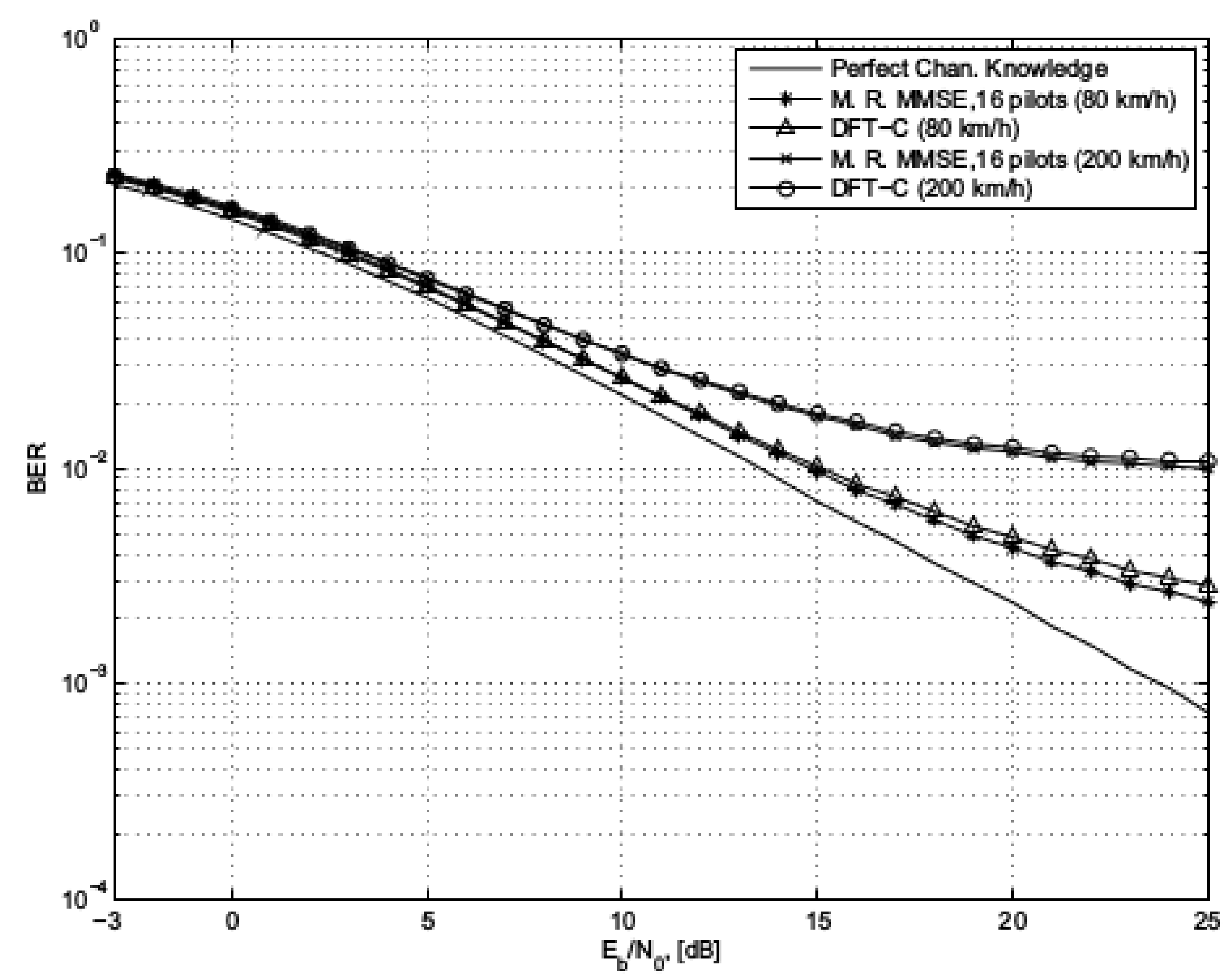

Fig. 13. DVB-H, uncoded BER performance for 4QAM corresponding to two different terminal speeds.

TABLE VI
DVB-H, ESTIMATOR COMPLEXITY, NUMBER OF REAL MULTIPLICATIONS PER OFDM SYMBOL

Estimator	Complexity
R. MMSE	2,661,648
M. R. MMSE	74,976
DFT-B	44,168
DFT-C	45,896

VII. CONCLUSION

In this paper, a number of novel methods have been proposed to address the channel estimation needs for a mobile terminal operating in a multistandard enviroment. Exploiting pilots in past/future symbols makes a core estimator plausible. The resultant pilot spacing for both LTE and DVB-H provides the opportunity to design a single estimator. These estimators have a relatively low computational complexity when compared to other investigated methods. The coexistence of these two low complexity estimators can provide the reliability and flexibility needed for the LTE as well as DVB-H systems. These estimators, however, lose their performance when significant changes in the enviroment (as a function of Doppler spread) occur specially for LTE. Considering the fact that UEs on average operate in a low terminal speed range as well as the reduced complexity which is gained by applying these estimation methods, the performance loss due to Doppler spread becomes acceptable in many situations. Meanwhile, these estimators perform well for relatively high terminal speeds when implemented for DVB-H which is mainly the result of the standardised pilot pattern as well as lower carrier frequency. Thus, the overall performance of these estimators when applied to fast fading channels becomes acceptable when both LTE and DVB-H are taken into consideration.

To improve the performance of these estimators for higher Doppler spreads in LTE, low complexity estimation techniques need to be applied to track the channel variations in time. Designing new estimators as such doesn't void the application of the proposed estimators in this paper. They will appear as added computational overhead which is due to time-domain filtering for LTE.

References

[1] M. Ozdemir and H. Arslan, "Channel estimation for wireless ofdm systems," *Communications Surveys & Tutorials, IEEE*, vol. 9, no. 2, pp. 18–48, 2007.

[2] P. Fertl and G. Matz, "Multi-user channel estimation in ofdma uplink systems based on irregular sampling and reduced pilot overhead," in *Acoustics, Speech and Signal Processing, 2007. ICASSP 2007. IEEE International Conference on*, vol. 3, pp. III–297–III–300, 2007.

[3] Ericsson, "White paper: Long term evolution (lte) an introduction," white paper, Ericsson AB, Oct. 2007.

[4] E. Dahlman, S. Parkvall, J. Skold, and P. Beming, *3G Evolution, Second Edition: HSPA and LTE for Mobile Broadband*. Academic Press, 2008.

[5] 3GPP, "Ts 36.213 v8.3.0 physical layer procedures," tech. rep., 3rd Generation Partnership Project, May 2008.

[6] ETSI, "Etsi en 300 744: Digital video broadcasting (dvb); framing structure, channel coding and modulation for digital terrestrial television (dvb-t)," tech. rep., ETSI, 2004.

[7] O. Edfors, *Low-complexity algorithms in digital receivers*. PhD thesis, Lulea University of Technology, September 1996.

[8] M. Gans, "A power-spectral theory of propagation in the mobile-radio environment," *Vehicular Technology, IEEE Transactions on*, vol. 21, no. 1, pp. 27–38, 1972.

[9] A. Goldsmith, *Wireless communications*. Cambridge University Press, 2005.

[10] M. Morelli and U. Mengali, "A comparison of pilot-aided channel estimation methods for ofdm systems," *Signal Processing, IEEE Transactions on*, vol. 49, no. 12, pp. 3065–3073, 2001.

[11] O. Edfors, M. Sandell, J.-J. van de Beek, S. K. Wilson, and P. O. Brjesson, "Analysis of dft-based channel estimators for ofdm," *Wireless Personal Communications*, vol. 12, no. 1, pp. 55–70, 2000.

[12] O. Edfors, M. Sandell, J.-J. van de Beek, S. Wilson, and P. O. Borjesson, "Ofdm channel estimation by singular value decomposition," in *Vehicular Technology Conference, 1996. 'Mobile Technology for the Human Race'., IEEE 46th*, vol. 2, pp. 923–927 vol.2, 1996.

[13] V. Srivastava, C. K. Ho, P. H. W. Fung, and S. Sun, "Robust mmse channel estimation in ofdm systems with practical timing synchronization," in *Wireless Communications and Networking Conference, 2004. WCNC. 2004 IEEE*, vol. 2, pp. 711–716 Vol.2, 2004.

[14] S. Omar, A. Ancora, and D. Slock, "Performance analysis of general pilot-aided linear channel estimation in lte ofdma systems with application to simplified mmse schemes," in *Personal, Indoor and Mobile Radio Communications, 2008. PIMRC 2008. IEEE 19th International Symposium on*, pp. 1–6, 2008.

[15] D. Takahashi and Y. Kanada, "High-performance radix-2, 3 and 5 parallel 1-d complex fft algorithms for distributed-memory parallel computers," *The Journal of Supercomputing*, vol. 15, pp. 207–228, Feb. 2000.

[16] D. Young and N. Beaulieu, "The generation of correlated rayleigh random variates by inverse discrete fourier transform," *Communications, IEEE Transactions on*, vol. 48, no. 7, pp. 1114–1127, 2000.